Molecular Level Characterization of Diatom and Coccolithophore-Associated Biopolymers That Are Binding ^{210}Pb and ^{210}Po in Seawater

Peng Lin[1]*, Chen Xu[1], Wei Xing[1] and Peter H. Santschi[1,2]

[1] Department of Marine and Coastal Environmental Science, Texas A&M University at Galveston, Galveston, TX, United States, [2] Department of Oceanography, Texas A&M University, College Station, TX, United States

Through a combination of selective extractions and molecular characterization techniques including Isoelectric Focusing Chromatography and Electrospray Ionization Fourier-Transform Ion Cyclotron Resonance Mass spectrometry, molecular structures of diatom (*Phaeodactylum tricornutum*) and coccolithophore (*Emiliania huxleyi*)-associated biopolymers that are responsible for the distinct partitioning behavior between ^{210}Pb and ^{210}Po were determined. Our results show that diatom-derived biopolymers have distinctive elemental grouping distributions as compared to those excreted by the coccolithophore, with the former consisting of more heterogeneous elements (i.e., nitrogen, sulfur and phosphorus-containing organic compounds). For the coccolithophore culture, two ^{210}Pb-enriched biopolymers (non-attached exopolymeric substances and coccosphere shell-associated biopolymers) have a higher abundance of CHO-type compounds, suggesting CHO-only-type compounds as the main binding moieties for ^{210}Pb. In contrast, such association was not evident in the diatom culture. Different with ^{210}Pb, ^{210}Po enrichment in coccolithophore-derived attached exopolymeric substances and Fe-Mn-associated metabolites coincided with the higher abundance of nitrogen/sulfur-containing organic compounds in these two biopolymer fractions, suggesting the strong parallel of Po with the production of nitrogen-rich organic matter as well as sulfur-containing amino acids. These different associations between ^{210}Pb/^{210}Po and organic functional groups were further explored by separating ^{210}Pb or ^{210}Po-labeled coccolithophore-derived biopolymers *via* isoelectric focusing. This technique suggests that phosphate group-containing molecules but not the other molecules that contain heterogeneous elements (e.g., CHONS, CHON, and CHOS) as the strongest binding agents for ^{210}Pb, while the more hydrophobic (high protein to carbohydrate ratio) nitrogen/sulfur-enriched organic moieties acted as the main ^{210}Po-binding ligands. It is concluded that the deficiency of ^{210}Po with respect to ^{210}Pb can be influenced by the relative abundance of nitrogen/sulfur-enriched organic moieties to the nitrogen/sulfur-depleted organic compounds in the water column. This behavior constrains the application of ^{210}Po-^{210}Pb approach to quantify the particulate organic

carbon (POC) export flux in the ocean. It also explains that differences in chemical binding of the ^{210}Po as compared to those of other radionuclides (e.g., thorium-234) as the main factor. That suggests that differences in decay half-lives or physical factors are less important when these nuclides are applied to estimate the POC flux in the ocean.

INTRODUCTION

Naturally occurring radionuclides with strong particle-reactivity, such as lead (Pb), polonium (Po), and thorium (Th), are widely used in estimating various biogeochemical and physical processes associated with marine particles in the ocean, mostly based on their strong particle reactivity and making use of disequilibria between parent and daughter radionuclides (e.g., Santschi et al., 1980; Anderson et al., 1983; Kumar et al., 1995; Murray et al., 2005; Stewart et al., 2010; Yang et al., 2011). Although most of these tracer applications are generally resting on inferences from correlations of isotopic ratios with bulk particle properties, experimental evidence reveals organic compound-specific scavenging and partitioning for different radionuclides, either in particulate or in colloidal phases (Hayes et al., 2015a,b; Lam et al., 2015; Lin et al., 2015). Furthermore, while previous focus was on inorganic matter as the main binding agents (e.g., opal, carbonate, and lithogenic; Chase et al., 2002; Guo et al., 2002; Roy-Barman et al., 2009; Lin et al., 2014), more recent experimental studies reveal the role of specific organic matter compounds in the scavenging of different radionuclides in marine environments (Roberts et al., 2009; Xu et al., 2011a; Chuang et al., 2014, 2015a,b; Lin et al., 2017).

In the global oceans, diatom and coccolithophores serve as the most important contributors to global oceanic primary production and to carbon flux (Nelson et al., 1995; Armbrust, 2009), whereby in-situ production and excretion of biogenic materials account for the majority of natural organic matter in the water column. During phytoplankton growth, secretion of fresh biopolymers (Chin et al., 1998; Santschi et al., 1998; Quigg et al., 2016) was shown to provide the strongest binding agents for different radionuclides compared with the naked diatom frustule (Chuang et al., 2014) or coccosphere (Lin et al., 2017, 2020). Furthermore, particle-reactive radionuclides can partition differently between diatom- and coccolithophore-predominated systems or among different biopolymer fractions of diatom or coccolithophore cells, which were attributed to different organic composition between different biopolymer fractions, and thus, to different affinities of the radionuclides to these fractions (Chuang et al., 2015b; Lin et al., 2017). However, the chemical composition of radionuclide-carrying biopolymer compounds derived from diatoms and coccolithophores are typically only quantified and characterized in terms of few groups of organic components, such as proteins, uronic acids, and carbohydrates. To fill this knowledge gap, the diatom *P. tricornutum* and coccolithophore *Emiliania huxleyi* were incubated for later separation of different biopolymer fractions, including extracellular fractions (non-attached and attached exopolymeric substances), frustule/coccosphere-associated biopolymers and intracellular biopolymers from cell lysis (Chuang et al., 2015b; Lin et al., 2017). In order to characterize the diatom/coccolithophore-derived biopolymers, specific organic compounds likely responsible for the scavenging and partitioning of ^{210}Pb and ^{210}Po in the water column, and examine their differences at the molecular level, Electrospray Ionization Fourier-Transform Ion Cyclotron Resonance Mass Spectrometry (ESI-FTICRMS) (Xu et al., 2020) was applied in the present study. In addition, different biopolymer fractions from coccolithophore were further labeled with ^{210}Pb and ^{210}Po, followed by the isoelectric focusing (IEF) gel electrophoresis and organic characterization of biopolymers enriched in the tracer radionuclides ^{210}Pb and ^{210}Po.

Considering the significant contribution of diatoms and coccolithophores to the carbon flux in the ocean, a better understanding on the association between radionuclides and organic components of diatom and coccolithophore-associated biopolymers can provide molecular level insights into the processes that control the oceanographic applications of natural radionuclides, such as the ^{210}Po-^{210}Pb pair, in predicting the organic carbon flux.

MATERIALS AND METHODS

Emiliania huxleyi and *Phaeodactylum tricornutum* Culturing

As described in Lin et al. (2017), natural seawater (pH = 8.0), collected from the Gulf of Mexico (Salinity = 35), was first filtered through a 0.2 μm polycarbonate cartridge to remove all particles, followed by cross-flow ultrafiltration using a 1 kDa cutoff membrane to remove colloidal organic matter (COM). Thus, the ultra-filterpassing fraction that contained only low-molecular-weight organic matter (<1 kDa), was then used as the culturing medium for the diatom *P. tricornutum* and coccolithophore *Emiliania huxleyi* species. After enrichment with f/2 medium nutrients, trace metals and vitamins, and sterilization, laboratory axenic *P. tricornutum* and *E. huxleyi* cultures were added to 100 mL of medium. All the incubations were conducted induplicates at 19 ± 1°C with a light:dark cycle of 14 h:10 h under an irradiation condition of 100 μmol-quanta/m^2/s. Additionally, a control cultures for each species were also set up to monitor the pH and growth status, measured as the change in optical density at 750 nm wavelength (OD$_{750}$) with a UV-Visspectrometer. Once the OD$_{750}$ value was constant, i.e., when the stationary phase for growth was reached, all cultures were harvested. Biopolymers were also sequentially extracted from the culture for the analysis of the biopolymer components (see details below).

Extracellular Biopolymer Extraction

The sequential chemical extraction scheme for obtaining individual fractions from *P. tricornutum* (**Supplementary Figure 1**) and *E. huxleyi* (**Supplementary Figure 2**) followed the procedures described in Chuang et al. (2015b) and Lin et al. (2017), with some modification. For the extracellular biopolymers excreted by the phytoplankton, non-attached exopolymeric substances (NAEPS) in the surrounding seawater and attached EPS (AEPS) associated with the cellular surface, were harvested. Laboratory cultures were centrifuged at 3,000 × *g* for 30 min, followed by filtration of the supernatant which was further concentrated and desalted with nanopure water (18.2 Ω) in 3 kDa Microsep centrifugal filter tubes (Milipore) to obtain the NAEPS fraction, while the resultant pellet from the centrifugation was resuspended by 50 mL 3% NaCl solution and stirred gently overnight at 4°C to extract EPS from the cellular surface. The solution was also centrifuged, and the supernatant containing the AEPS was then filtered to remove residual cells before further desalting *via* the 3 kDa ultrafiltration centrifugation tubes. The final volume of concentrated solution of each biopolymer fraction (>3 kDa) was 2 mL.

Extraction of *Phaeodactylum tricornutum* Intracellular Biopolymers and Its Frustule-Related Biopolymers

Given the different shells for these two phytoplankton species (silica frustule for the diatom *P. tricornutum* and biogenic calcite for the coccolithophore *E. huxleyi*), sequential extraction procedures were applied to access the intracellular and frustule/coccosphere associated biopolymers in *P. tricornutum* and *E. huxleyi* cells, respectively (**Supplementary Figures 1, 2**). For the *P. tricornutum* cultures, 10 mL of 100 mM EDTA (pH 8.0) solution was added to the diatom cells from the previous AEPS extraction step. The diatom cells were resuspended at 4°C overnight to extract the intracellular material after diatom cell lysis and the supernatant was collected after centrifugation to obtain the EDTA-extractable intracellular biopolymers (EDTA-intracellular, **Supplementary Figure 1**). Then, the resultant pellet was further resuspended in 10 mL of 1% SDS/10 mM Tris (pH 6.8) solution and heated at 95°C for 1 h. The centrifuged supernatant was also collected and defined as SDS-extractable intracellular biopolymer (SDS-intracellular, **Supplementary Figure 1**) in *P. tricornutum* cells.

To access the diatom frustule-associated biopolymers (Frustule-BP, **Supplementary Figure 1**), 5 mL of 52% HF was then added to the frustules and incubated on ice for 1 h. After the separation of the HF-insoluble pellet, the HF-soluble fraction was evaporated under N$_2$ stream and neutralized, followed by 3 kDa centrifugal filtration to collect the digested frustule silica fraction (<3 kDa) and HF-soluble frustule-associated biopolymer (>3 kDa). Lastly, the residual biopolymer in the HF-insoluble pellet was collected by resuspension in a 2 mL of 100 mM ammonium acetate solution and sonication. Similar to NAEPS and AEPS, all the *P. tricornutum* cellular biopolymers were concentrated and desalted with nanopure water in 3 kDa Microsep centrifugal filter tubes (Milipore).

Emiliania huxleyi Coccosphere (Biogenic Calcite) and Biopolymer Extraction

The coccosphere of the *E. huxleyi* cells was first dissolved before the extraction of intracellular biopolymers. In brief, the pellet from the previous AEPS extraction step was digested in 0.44 M acetic acid (HAc) (weak acidity and non-oxidizing nature to avoid the breakage of cells) plus 0.1 M NaCl solution at 4°C for 8 h. After the digestion, the mixed solution was centrifuged and filtered, followed by ultrafiltration of the supernatant with 3 kDa Microsep centrifugal filter tubes. The retentate (>3 kDa) was defined as coccosphere-associated biopolymers (Shell-BP, **Supplementary Figure 2**).

The *E. huxleyi* cells after the removal of shells were further heated in 20 mL of 1% SDS/10 mM Tris mixed solution (pH 6.8) at 95°C for 1 h. The supernatant was also collected by centrifugation and filtration, followed by desalting with 3 kDa Microsep centrifugal filter tubes. Subsequently, the remaining pellet was further digested by 0.04 M NH$_2$OH·HCl/4.35 M HAc mixture at 96°C for 6 h to obtain the intracellular metabolitic biopolymer. These two fractions (Intracellular and Fe, Mn-BP, **Supplementary Figure 2**) can represent the intracellular biopolymers in *E. huxleyi* cells.

Lastly, it should be noted that the parallel ^{210}Pb/^{210}Po-labeled diatom and coccolithophore incubation experiments have been described in Chuang et al. (2015b) and Lin et al. (2017), whose data (**Supplementary Figures 3, 4**) were used in the present study to examine the association between ^{210}Pb/^{210}Po partitioning and organic characterization in various biopolymer fractions.

Isoelectric Focusing of Radionuclide-Labeled Biopolymer

Different fractions of purified *E. huxleyi*-derived biopolymers were incubated individually with ^{210}Pb and ^{210}Po (total activity at 250 Bq, respectively, equivalent to 50 fMoles, considerably lower than ambient Pb/Po concentration), respectively, in nanopure water (18.2 Ω), followed by subsequent isoelectric focusing (IEF) gel electrophoresis to determine the pH$_{IEF}$ of potential binding ligands for each radionuclide (Alvarado Quiroz et al., 2006; Chuang et al., 2014). This was to further examine the organic compounds binding the majority of each radionuclide in each biopolymeric fraction. After IEF separation, the strip was then cut into 11 1-cm pieces and measured for the radionuclide activities in each pH section, through gamma spectrometry (^{210}Pb at 46.3 kev) and liquid scintillation counting (^{210}Po). The samples were counted for enough time to obtain the activity error < 10%, with the detection limit of 0.05 Bq for ^{210}Pb (based on at least 1-day counting) and 0.5 Bq for ^{210}Po, respectively. The pH section, which contained the highest activity of radionuclide was cut from the IEF gel of the non-radiolabeled biopolymers and extracted with 1% sodium dodecyl sulfate (SDS) solution for 2 days, and is called here the "IEF extract." Similar to the bulk biopolymer fraction, these radionuclide-enriched "IEF extracted" biopolymer fractions were diafiltered with nanopure water through 3 kDa Microsep centrifugal filter tubes, to remove all electrophoresis reagents and SDS that would otherwise interfere with later ESI-FTICRMS analysis.
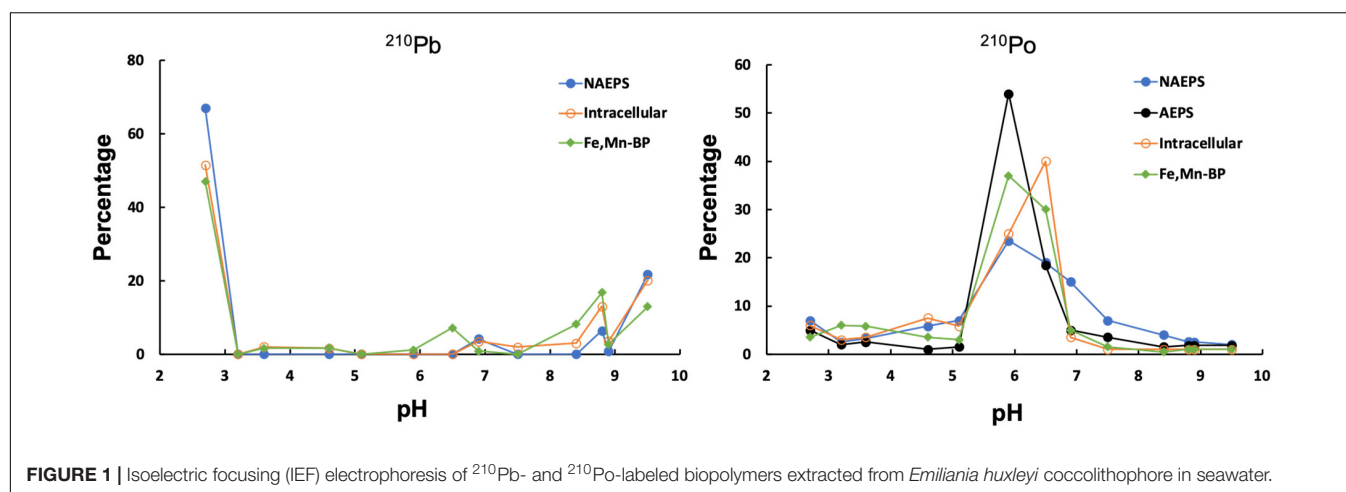
FIGURE 1 | Isoelectric focusing (IEF) electrophoresis of ^{210}Pb- and ^{210}Po-labeled biopolymers extracted from *Emiliania huxleyi* coccolithophore in seawater.

ESI-FTICRMS Analysis

All the *E. huxleyi*-derived biopolymers, including the bulk and IEF-fractionated fractions, were freeze-dried, re-dissolved in nanopure water, mixed with methanol at a 1:1 ratio, and analyzed by electrospray ionization Fourier-transform ion cyclotron resonance mass spectrometry (ESI-FTIRCMS) in the negative mode (Xu et al., 2015, 2020), at the College of Sciences Major Instrumentation Cluster, Old Dominion University, Virginia. The procedural blank, which went through all isotope incubation and IEF gel electrophoresis experiment steps, was analyzed at the same time. Samples were injected using a Hamilton syringe at a flow rate of 2 μL/min into the Apollo II ESI ion source of a Bruker Daltonics 12 Tesla Apex Qe FTICRMS. The coated glass capillary temperature was set to 200°C and the electrospray voltages were optimized to keep the ion current constant. The ion accumulation time was set to 2.0 s and 200 scan averages were co-added between 100 and 1,000 m/z.

Mass spectra were internally calibrated using a series of reference organic acids. Formula calculation was accomplished using a molecular formula calculator (Molecular Formula Calc. v. 1.1 NHMFL) developed at the national High Magnetic Field Laboratory in Tallahassee, FL, using peaks with a signal-to-noise (S/N) ratio of $\geq$ 4, a m/z range between 200 and 900, and a mass error less than 1.0 ppm. The following criteria were used for formula assignment: C_{6-75}, H_{2-100}, N_{0-8}, O_{0-35}, S_{0-4}, and P_{0-1}. All formulas were screened to eliminate those that are unlikely to occur in NOM, according to a list of selection criteria (Stubbins et al., 2010). Procedure blanks peaks were removed from the final formula list. Peaks with multiple possible formulas (usually those peaks with m/z values > 400 Da) were assigned formulas through the detection of homologous series (CH_2, COO, O_2, C_2H_4O, H_2, etc.). Molecular formulas were lastly screened by searching chemical structures in the Pubchem database[1]. Formulas with no chemical structures identified in the Pubchem database were excluded from the final formula assignment.

Aromatic compounds and condensed aromatic compounds were assigned to formulas with aromaticity indices [AI, calculated

by (1+C-0.5O-S-0.5H)/(C-0.5O-S-N-P)] greater than 0.5 and 0.67, respectively. The double bond equivalent (DBE) was calculated as DBE = 1+ 0.5 (2C-H+N+P). Aliphatic compounds were assigned to formulas DBE: C < 0.3 and H:C = 1.0–3.0. The carboxyl-containing aliphatic (number of COO-R functionality $\geq$ 1) and/or alicyclic molecules (CCAM) were assigned to formulas with H:C of 0.85–2.00 and O:C of 0–0.40.

RESULTS AND DISCUSSION

pH Gradient of Radionuclides in Isoelectric Focusing

Distributions of ^{210}Pb and ^{210}Po bound by coccolithophore-derived biopolymers, along the IEF-pH gradient, are shown in **Figure 1**. The results clearly indicate that Po and Pb radionuclides selectively bind with coccolithophore biopolymers of distinctly different IEF points (pH$_{IEF}$) where a compound class has a zero net surface charge. This compound class contains specific functional groups for binding the ^{210}Pb and ^{210}Po. For ^{210}Pb, about 50% of labeled SDS-extractable intracellular biopolymers and intracellular Fe-Mn-associated metabolites was found below pH of 3, with a minor fraction concentrated above pH of 8. For labeled NAEPS, more than 60% of ^{210}Pb was detected below pH of 3. Such ^{210}Pb-IEF pH profiles are the opposite of the observed patterns for the ^{210}Pb-labeled diatom-derived biopolymers showing the majority of ^{210}Pb distributing above pH of 9 (Chuang et al., 2014), probably due to different compositions and specific functional groups between diatom- and coccolithophore-derived biopolymers (see sections below).

In contrast, results from the pH gradient of ^{210}Po-labeled coccolithophore-derived biopolymers demonstrated similar profiles as the observation in diatom-derived biopolymers (Chuang et al., 2014), as discussed below. As shown in **Figure 1**, all the ^{210}Po-labeled biopolymers showed a main pH$_{IEF}$ peak between pH 6–7. Overall, it is evident that ^{210}Pb and ^{210}Po showed different patterns in their IEF profiles (**Figure 1**), demonstrating that these two radionuclides are bound to different types of organic functional groups in

---

[1]https://pubchem.ncbi.nlm.nih.gov/search

individual biopolymers from the coccolithophore. ^{210}Pb seemed to be complexed mainly by negatively charged organic macromolecules, while neutral organic functional groups are responsible for the binding of ^{210}Po.

Different Molecular Compositions of Diatom- and Coccolithophore-Derived Biopolymers Associated With Radionuclide Partitioning

Distribution of various molecular formula types among different biopolymer fractions in diatom and coccolithophore cultures were identified through the generation of a van Krevelen diagram of all formulas (**Figure 2**), and their elemental groupings for bulk organic matter from the two species are displayed in **Figure 3**. It is evident that diatom-derived biopolymers have different distinct elemental grouping distributions compared to those excreted by coccolithophore, with the former consisting of more heterogeneous elements (i.e., nitrogen, sulfur and phosphorus-containing groups). For example, coccolithophore-derived NAEPS consisted primarily of CHO formulas (68% by number and 58% by intensity) and had minor abundance of CHONS-only and phosphorus-containing compounds (both < 10%), while CHONS-type (31% by number and 28% by intensity) and phosphorus-containing compounds (20% by number and 30% by intensity) were both predominant formula types in diatom-derived NAEPS. Additionally, individual diatom-derived biopolymer fractions had a relatively more homogeneous distributions in elemental grouping (e.g., 15–25% for all molecular formula type in AEPS), compared to coccolithophore, showing a higher concentration in specific molecular formula types for an individual biopolymer fraction (e.g., >80% as CHOS in intracellular Fe-Mn-associated metabolites, **Figure 3**).

Such significant differences in the molecular composition of these biopolymers of the two phytoplankton species can explain our previously observed different partitioning of ^{210}Pb or ^{210}Po in biopolymers derived from diatom and coccolithophore (**Supplementary Figures 3, 4**, also reported in Chuang et al., 2015b; Lin et al., 2017). In coccolithophore cultures, ^{210}Pb was mostly concentrated in the coccosphere shell (∼65%), with a minor abundance in shell-associated biopolymers and moderate abundance in NAEPS (∼30%). None of ^{210}Pb can pass through the coccosphere shell to the intracellular fraction (**Supplementary Figure 3**). In contrast, ^{210}Pb can be detected in all diatom-derived biopolymers. It showed relatively even amounts of ^{210}Pb in three main diatom-derived biopolymer fractions (i.e., exopolymeric substances (NAEPS+AEPS) vs. frustule-associated biopolymer vs. intracellular biopolymer, **Supplementary Figure 4**), ranging from 20 to 35% (**Supplementary Figure 4**). Together, ^{210}Pb distribution patterns seemed to coincide with the distribution pattern of elemental groupings as mentioned above for coccolithophores and diatoms. Specifically, for the coccolithophore, higher enrichment in CHO-type compounds in NAEPS and coccosphere shell-associated biopolymers coincided with their higher enrichment in ^{210}Pb (**Supplementary Figure 3**), suggesting that CHO-only-type compounds are

the main moieties binding ^{210}Pb in the coccolithophore. However, substituting of ^{210}Pb for Ca^{2+} during coccolith formation seemed to prevent the uptake of ^{210}Pb by intracellular biopolymers that were also enriched in CHO-type moieties, as reflected in a CHO-only compound-dominant in the intracellular biopolymer (**Figure 3**), yet ∼0% of the amended ^{210}Pb was found (**Supplementary Figure 3**; Lin et al., 2017). In contrast, the diatom frustule (i.e., biogenic silica) does not have such a "shielding" effect for the intracellular uptake of ^{210}Pb. Therefore, considerable and relatively even activity of ^{210}Pb can be detected among exopolymeric substances, frustule-associated biopolymer and intracellular biopolymer (**Supplementary Figure 4**). The apparent "non-specific" binding of ^{210}Pb in diatom-associated biopolymer fractions as well as the diatom frustule suggests that the responsible ^{210}Pb binding moieties have a more homogeneous distribution in diatom species.

Different from ^{210}Pb, ^{210}Po can be detected in various coccolithophore-derived biopolymers, especially in the AEPS and intracellular Fe-Mn-associated metabolites (**Supplementary Figure 3**). Together with the distribution of molecular formula types (**Figure 3**), we can easily find that the ^{210}Po-enriched APES and Fe-Mn-associated metabolites both have higher abundance of nitrogen/sulfur-containing organic compounds (e.g., >40% as CHONS for AEPS and >80% as CHOS for Fe-Mn-associated metabolites), in agreement with the binding properties of Po, i.e., being preferentially related to the production and distribution of nitrogen-rich organic matter as well as sulfur-containing amino acids (Stewart et al., 2007b). Although the Po partitioning among different diatom-derived biopolymers was not investigated in the present study, we may expect stronger association of Po with diatom-derived biopolymers considering the more heterogeneous organic compounds produced by the diatom (i.e., N and S-containing compounds).

Overall, distinct molecular compositions between diatom- and coccolithophore-derived biopolymers not only result in considerable differences in radionuclide partitioning [e.g., ^{210}Pb, Lin et al. (2017) vs. Chuang et al. (2015b)] between diatoms and coccolithophores, but also contribute to the possible fractionation between radionuclides in diatom- vs. coccolithophore-dominated marine environments (see sections below).

Radionuclide-Carrying Moieties in Coccolithophore-Derived Biopolymers

Since the isoelectric points are unique for the different radionuclides as shown in **Figure 1**, it suggests that specific organic carrier moieties are responsible for the binding of individual radionuclides in the coccolithophore. Thus, the molecular compositions of the Pb/Po-enriched macromolecules were further explored through IEF separation of different coccolithophore-derived biopolymers and characterization by ESI-FTICRMS.

Among five biopolymers, only two fractions of biopolymers, including NAEPS and coccosphere shell-associated biopolymers, have the capability to strongly bind the ^{210}Pb (**Supplementary Figure 3**; Lin et al., 2017). Nevertheless, IEF sections of
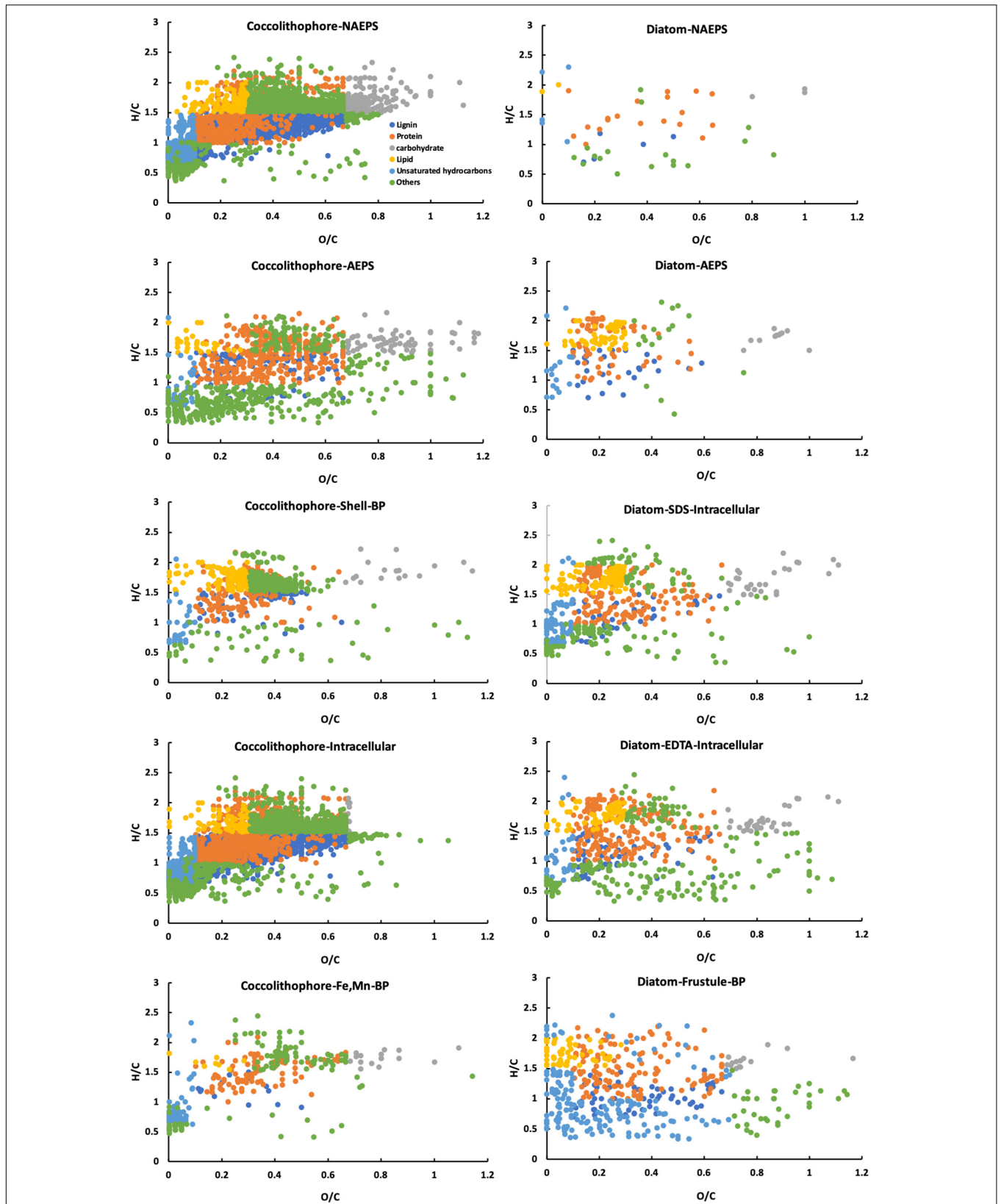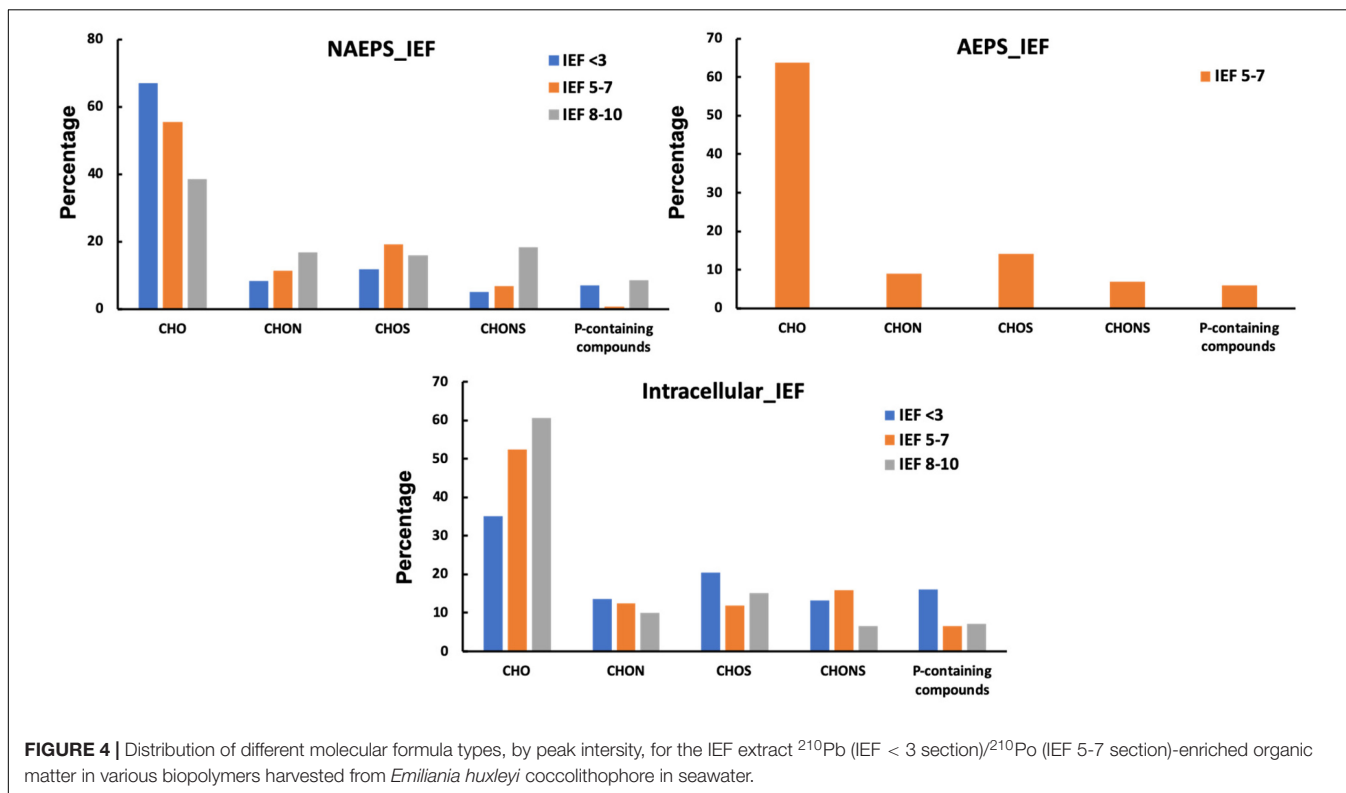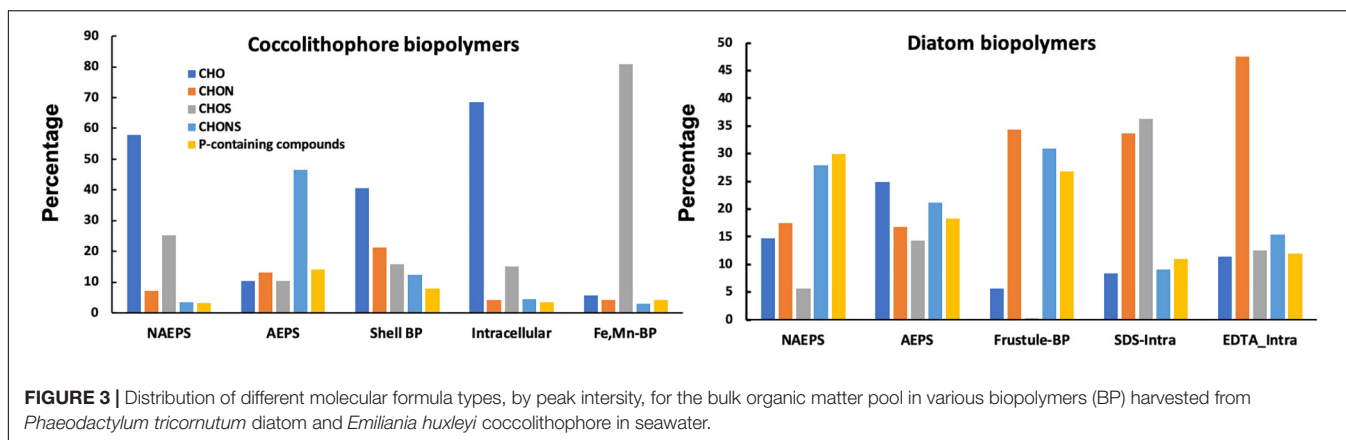
FIGURE 2 | van Krevelen diagram showing all formulas and molecular classes for various biopolymers (BP) excreted by *Emiliania huxleyi* coccolithophore and *Phaeodactylum tricornutum* diatom in seawater.

FIGURE 3 | Distribution of different molecular formula types, by peak intersity, for the bulk organic matter pool in various biopolymers (BP) harvested from *Phaeodactylum tricornutum* diatom and *Emiliania huxleyi* coccolithophore in seawater.

FIGURE 4 | Distribution of different molecular formula types, by peak intersity, for the IEF extract ^{210}Pb (IEF < 3 section)/^{210}Po (IEF 5-7 section)-enriched organic matter in various biopolymers harvested from *Emiliania huxleyi* coccolithophore in seawater.

coccosphere shell-associated biopolymers are not presented here due to limitations in sample availability for FTICR-MS analysis and relatively minor partitioning of ^{210}Pb in this biopolymer fraction (<5%). For NAEPS, the CHO-only functional group consistently decreased from 67 to 39% along the IEF pH gradient from anode (NAEPS IEF < 3) to the cathode (NAEPS IEF 8–10), whereas nitrogen- or sulfur-containing organic compounds (i.e., CHON+CHONS or CHOS+CHONS) increased from low to high pH sections (**Figure 4**). Furthermore, it is notable that phosphorus enrichment can be seen along with the ^{210}Pb augmentation of NAEPS-"IEF extracts" (i.e., IEF < 3, **Figure 4**) based on our elemental ratio results, showing a 2–3 fold increase in phosphorus to carbon ratio for ^{210}Pb-enriched IEF < 3 sub-fraction of NAEPS compared with that in the bulk NAEPS

(**Supplementary Table 1** phosphorus% and phosphorus:carbon ratio in the bulk NAEPS as 0.21% and $1.50*10^{-3}$ vs. those as $0 \times 54\%$ and 3.97×10^{-3} in the IEF < 3 sub-fraction, respectively). Together, these phosphorus-containing molecules but not the other molecules that contain heterogeneous elements (e.g., CHONS, CHON, and CHOS) stand out as the main binding moieties for ^{210}Pb in the coccolithophore-dominated systems. Considering the majority of ^{210}Pb complexed by negatively charged organic macromolecules (**Figure 1**), our IEF observational results may allow us to consider that these phosphorus-containing molecules can be composed of abundant phosphate functional groups (e.g., Karl, 2014; Albi and Serrano, 2016), consequently serving as the main ^{210}Pb-binding ligands in the coccolithophore-dominated marine environments.

For the ^{210}Po, its major peak along the IEF sections was identified at pH 6 (i.e., pH between 5 and 7, **Figures 1, 4**) for the coccolithophore-derived biopolymers. All the biopolymer fractions, excluding coccosphere shell-associated biopolymer, have the capability to bind ^{210}Po in seawater (**Supplementary Figure 3**). The IEF 5-7 section were then further processed for the molecular compositional analysis, except for Fe-Mn-associated metabolites due to the limitation of sample availability. Notably, N enrichment can be seen with the Po enriched fraction of both "IEF extract" for NAEPS (11–18%) and intracellular biopolymers (9–28%), while the sulfur enrichment can be only found in the "IEF extract" of intracellular biopolymers (20–27%) of the coccolithophore. However, neither N nor sulfur enrichment was seen for the "IEF extract" of the AEPS. Instead, the abundance of nitrogen/sulfur-containing groups evidently decreased in AEPS-"IEF extract" (60–16% for N and 57–28% for sulfur). This is likely due to the fact that the only portion of nitrogen/sulfur-rich organic compounds in the bulk AEPS contain specific ligands that can strongly bind Po from the seawater, e.g., neutrally charged amphiphilic protein-containing compounds. Other nitrogen/sulfur-rich organic compounds in the bulk AEPS were concentrated in other IEF sections, e.g., the negatively charged acid polysaccharide containing the sulfate functional groups. This can be further confirmed by the difference in the molecular class information between the "IEF extract" and the bulk biopolymers (**Table 1**). For example, strong enrichment in protein-containing compounds can be seen along with the ^{210}Po augmentation of intracellular biopolymer-"IEF extracts," coincidence with the intensified relative hydrophobicity of Po-carrying macromolecules based on the ratio of protein to carbohydrate (Xu et al., 2011b). Although the protein abundance in "IEF extract" of both extracellular biopolymers (i.e., NAEPS and AEPS) decreased compared with the bulk extracellular biopolymers, the nature of their Po-carrying moieties became relatively more hydrophobic along the pH gradient in the IEF gel (e.g., four times increase in protein/carbohydrate ratio for NAEPS IEF anode as 3.56 to IEF pH 5-7 as 11.35, **Table 1**). Therefore, these results provide direct evidence supporting the hydrophobic nitrogen/sulfur-enriched organic moieties, either within colloidal extracellular pool or within particulate intracellular pool, serving as the strongest binding agents for Po scavenging in the coccolithophore-dominated marine environments. Higher protein/carbohydrate ratios of EPS are indicators of their "stickiness" or propensity for aggregate formation (Santschi et al., 2020). Furthermore, this further confirmed the distinct organic-binding nature of the ^{210}Po carrier compounds, as compared with to its parent nuclide, ^{210}Pb, which could strongly affect their scavenging and their tracing application in the ocean.

Implications for the Application of ^{210}Pb and ^{210}Po

Based on the ^{210}Po deficiency with respect to ^{210}Pb, they have been widely used as radionuclide tracer pair to quantify the particulate organic carbon (POC) export from the upper water column to deeper ocean. Nevertheless, as mentioned above, ^{210}Pb in coccolithophore dominated algae culture would be not only preferentially scavenged by coccoliths (**Supplementary Figure 3**), but also have distinct affinity

TABLE 1 | Molecular class information and its individual distribution percentage for the bulk biopolymers (BP) and corresponding "IEF extract" Pb-enriched- (IEF < 3) or Po-enriched- (IEF 5-7) organic matter in the coccolithophore culture, as well as for the bulk biopolymers in the diatom culture, as revealed by ESI-FTICRMS.

	Lignin	Protein	Carbohydrate	Lipids	Unsaturated hydrocarbon	Others	Carboxyl-rich alicyclic molecules (CRAM)	Protein-C/Carbohydrate-C ratio*
Coccolithophore (*Emiliania huxleyi*)								
NAEPS	20.79	10.46	4.92	1.80	24.15	37.87	10.50	2.82
AEPS	5.38	22.61	4.97	0.65	1.99	64.38	15.49	6.02
Shell-BP	8.91	27.95	2.37	14.70	6.74	39.33	16.79	15.61
Intracellular	18.95	9.02	7.98	1.34	34.85	27.86	10.00	1.50
Fe, Mn-BP	0.99	9.70	1.03	11.20	4.73	72.35	4.63	12.43
Coccolithophore (*Emiliania huxleyi*)-IEF								
NAEPS-IEF < 3	49.76	9.33	3.47	11.21	3.67	22.57	10.29	3.56
NAEPS-IEF 5-7	52.71	10.49	1.22	3.69	2.73	29.16	16.25	11.35
AEPS-IEF 5-7	58.58	9.48	1.67	8.13	2.60	19.55	9.74	7.54
Intracellular-IEF 5-7	52.94	19.64	1.35	6.11	2.88	17.08	14.62	19.23
Diatom (*Phaeodactylum tricornutum*)								
NAEPS	10.52	45.59	5.40	2.11	5.31	31.08	26.63	11.19
AEPS	11.97	25.86	13.73	33.16	5.67	9.60	8.99	2.50
SDS-intracellular	4.62	36.10	2.29	10.50	7.52	38.97	30.79	20.88
EDTA-intracellular	10.23	58.36	3.65	5.49	1.90	20.36	51.40	21.16
Frustule-BP	10.42	48.93	9.02	8.61	19.59	3.42	13.58	7.18

*Protein to carbohydrate ratio, using the value in "Protein" column multiplied by 0.53 (the average carbon content in protein) divided by the product of the value in "Carbohydrate" column and 0.4 (the average carbon content in carbohydrate).

and selectivity to the organic functional groups, compared with ^{210}Po. Thus, the deficiency of ^{210}Po with respect to ^{210}Pb may limit the quantification of the POC export fluxes under certain situations (Friedrich and Rutgers van der Loeff, 2002; Stewart et al., 2005; Lin et al., 2017), specifically when more hydrophobic nitrogen/sulfur-enriched organic moieties are enriched (preferentially scavenge ^{210}Po) or where biogenic carbonate particles (i.e., incorporation of ^{210}Pb into coccosphere shell) are abundant. Instead, when biogenic carbonate is not abundant (e.g., diatom-dominated environments), the deficiency of ^{210}Po with respect to ^{210}Pb may actually reflect the relative abundance of nitrogen/sulfur-enriched organic moieties (e.g., protein for ^{210}Po) to the nitrogen/sulfur-depleted organic compounds (e.g., polysaccharides for ^{210}Pb) in the water column. Thus, the investigation on the particle composition, including inorganic (e.g., abundance of biogenic carbonate) and organic compound characterization, may help us distinguish if the ^{210}Pb/^{210}Po disequilibrium can be applied or not for the POC export estimation. Specific correction of the ^{210}Pb/^{210}Po disequilibrium based on the variation in the particle composition in the water column (e.g., vertical profile of particulate protein to polysaccharide ratio) may increase the accuracy of this radionuclide pair for the POC export estimation.

Similarly, this may also explain the different estimated POC export fluxes in the same oceanic regions between several radionuclide-pair tracing approaches, such as ^{234}Th/^{238}U vs. ^{210}Po/^{210}Pb (Verdeny et al., 2009; Stewart et al., 2011; Le Moigne et al., 2013). Different selectivity to the organic matter between ^{234}Th (e.g., selectivity to negatively charged functional groups, like acid polysaccharide; Guo et al., 2002; Quigley et al., 2002; Lin et al., 2015) and ^{210}Po may be biasing the corresponding POC export flux estimates. For example, a higher ^{234}Th-derived POC flux than ^{210}Po-derived POC flux may potentially resulting from the higher abundance of acid polysaccharide-like compounds relative to more amphiphilic nitrogen/sulfur-rich organic compounds (e.g., proteins) in the bulk organic matter pool. Therefore, a combination of the organic compound characterization with the application of radionuclides may help us better understand biases in the estimates of the export fluxes of the particulate organic matter in the ocean by providing a firmer confirmation of earlier suggestions of the preference of ^{210}Po for binding to compounds in the cytoplasm (Friedrich and Rutgers van der Loeff, 2002). In particular, it provides a better foundation to the earlier suggestion by Friedrich and Rutgers van der Loeff (2002) of strong ^{210}Po binding to diatoms. Our study also provides primary evidence that distinct organic matter compounds are responsible when the ^{210}Po/^{210}Pb approach in field-based POC flux estimations significantly differ

from estimates by other approaches, e.g., using ^{234}Th/^{238}U disequilibria (Shimmield et al., 1995; Friedrich and Rutgers van der Loeff, 2002; Stewart et al., 2007a, 2011; Verdeny et al., 2009; Wei et al., 2011; Anand et al., 2018). Field studies at best provide correlations, but intrinsically suffer from hiding unequivocal causal relationships. Thus, when different approaches to POC flux estimations were carried out, significant differences in the results usually could not distinguish between different causes, e.g., time scales (half-lives of tracers, 24 days for ^{234}Th and 138 days for ^{210}Po), physical factors (Moran et al., 2003), and differences in organic matter ligand moieties.

DATA AVAILABILITY STATEMENT

The original contributions presented in the study are included in the article/**Supplementary Material**, further inquiries can be directed to the corresponding author/s.

AUTHOR CONTRIBUTIONS

PL, CX, and PS conceived and designed the experiment and wrote the manuscript. PL and WX performed the incubation and partitioning experiment. PL performed the organic matter extraction. PL, CX, and WX performed the data processing. All authors contributed to the article and approved the submitted version.

FUNDING

ACKNOWLEDGMENTS

SUPPLEMENTARY MATERIAL

The Supplementary Material for this article can be found online at: https://www.frontiersin.org/articles/10.3389/fmars.2021.703503/full#supplementary-material

REFERENCES

Albi, T., and Serrano, A. (2016). Inorganic polyphosphate in the microbial world. Emerging roles for a multifaceted biopolymer. *World J. Microbiol. Biotechnol.* 32:27.

Alvarado Quiroz, N. G., Hung, C.-C., and Santshi, P. H. (2006). Binding of thorium(IV) to carboxylate, phosphate and sulfate functional groups from marine exopolymeric substances (EPS). *Mar. Chem.* 100, 337–353. doi: 10.1016/j.marchem.2005.10.023

Anand, S. S., Rengarajan, R., Shenoy, D., Gauns, M., and Naqvi, S. W. A. (2018). POC export fluxes in the Arabian Sea and the Bay of Bengal: a simultaneous ^{234}Th/^{238}U and ^{210}Po/^{210}Pb study. *Mar. Chem.* 198, 70–87.

Anderson, R. F., Bacon, M. P., and Brewer, P. G. (1983). Removal of ^{230}Th and ^{231}Pa at ocean margins. *Earth Planet. Sci. Lett.* 66, 73–90.

Armbrust, E. V. (2009). The life of diatoms in the world's oceans. *Nature* 459, 185–192. doi: 10.1038/nature08057

Chase, Z., Anderson, R. F., Fleisher, M. Q., and Kubik, P. W. (2002). The influence of particle composition and particle flux on scavenging of Th, Pa and Be in the ocean. *Earth Planet. Sci. Lett.* 204, 215–229. doi: 10.1016/s0012-821x(02)00984-6

Chin, W. C., Orellana, M. V., and Verdugo, P. (1998). Spontaneous assembly of marine dissolved organic matter into polymer gels. *Nature* 391, 567–571.

Chuang, C.-Y., Santschi, P. H., Jiang, Y., Ho, Y.-F., Quigg, A., Guo, L., et al. (2014). Important role of biomolecules from diatoms in the scavenging of particle-reactive radionuclides of thorium, protactinium, lead, polonium and beryllium in the ocean: a case study with *Phaeodactylum tricornutum. Limnol. Oceanogr.* 59, 1256–1266. doi: 10.4319/lo.2014.59.4.1256

Chuang, C.-Y., Santschi, P. H., Wen, L.-S., Guo, L., Xu, C., Zhang, S., et al. (2015a). Binding of Th, Pa, Pb, Po and Be radionuclides to marine colloidal macromolecular organic matter. *Mar. Chem.* 173, 320–329. doi: 10.1016/j.marchem.2014.10.014

Chuang, C.-Y., Santschi, P. H., Xu, C., Jiang, Y., Ho, Y.-F., Quigg, A., et al. (2015b). Molecular level characterization of diatom-associated biopolymers that bind ^{234}Th, ^{233}Pa, ^{210}Pb, and ^{7}Be in seawater: a case study with *Phaeodactylum tricornutum. J. Geophys. Res. Biogeosci.* 120, 1858–1869. doi: 10.1002/2015jg002970

Friedrich, J., and Rutgers van der Loeff, M. M. (2002). A two-tracer (^{210}Po-^{234}Th) approach to distinguish organic carbon and biogenic silica export flux in the Antarctic circumpolar current. *Deep Sea Res. I* 49, 101–120. doi: 10.1016/s0967-0637(01)00045-0

Guo, L., Chen, M., and Gueguen, C. (2002). Control of Pa/Th ratio by particulate chemical composition in the ocean. *Geophys. Res. Lett.* 29:1961.

Hayes, C. T., Anderson, R. F., Fleisher, M. Q., Huang, K.-F., Robinson, L. F., Lu, Y., et al. (2015a). ^{230}Th and ^{231}Pa on GEOTRACES GA03, the U.S. GEOTRACES North Atlantic transect, and implications for modern and paleoceanographic chemical fluxes. *Deep Sea Res. I Top. Stud. Oceanogr.* 116, 29–41. doi: 10.1016/j.dsr2.2014.07.007

Hayes, C. T., Anderson, R. F., Fleisher, M. Q., Vivancos, S. M., Lam, P. J., Ohnemus, D. C., et al. (2015b). Intensity of Th and Pa scavenging partitioned by particle chemistry in the North Atlantic Ocean. *Mar. Chem.* 170, 49–60. doi: 10.1016/j.marchem.2015.01.006

Karl, D. M. (2014). Microbially mediated transformations of phosphorus in the sea: new views of an old cycle. *Annu. Rev. Mar. Sci.* 6, 279–337. doi: 10.1146/annurev-marine-010213-135046

Kumar, N., Anderson, R. F., Mortlock, R. A., Froelich, P. N., Kubik, P., Dittrich-Hannen, B., et al. (1995). Increased biological productivity and export production in the glacial Southern Ocean. *Nature* 378, 675–680. doi: 10.1038/378675a0

Lam, P. J., Ohnemus, D. C., and Auro, M. E. (2015). Size-fractionated major particle composition and concentrations from the US GEOTRACES North Atlantic Zonal Transect. *Deep Sea Res. II Top. Stud. Oceanogr.* 116, 303–320. doi: 10.1016/j.dsr2.2014.11.020

Le Moigne, F. A. C., Villa-Alfageme, M., Sanders, R. J., Marsay, C., Henson, S., and Garcia-Tenorio, R. (2013). Export of organic carbon and biominerals derived from ^{234}Th and ^{210}Po at the Porcupine Abyssal Plain. *Deep Sea Res. I Oceanogr. Res. Papers* 72, 88–101. doi: 10.1016/j.dsr.2012.10.010

Lin, P., Chen, M., and Guo, L. (2015). Effect of natural organic matter on the adsorption and fractionation of thorium and protactinium on nanoparticles in seawater. *Mar. Chem.* 173, 291–301. doi: 10.1016/j.marchem.2014.08.006

Lin, P., Guo, L., and Chen, M. (2014). Adsorption and fractionation of thorium and protactinium on nanoparticles in seawater. *Mar. Chem.* 162, 50–59. doi: 10.1016/j.marchem.2014.03.004

Lin, P., Xu, C., Xing, W., Sun, L., Schwehr, K. A., Quigg, A., et al. (2020). Partitioning of iron and plutonium to exopolymeric substances and intracellular biopolymers: a comparison study between the coccolithophore *Emiliania huxleyi* and the diatom *Skeletonema costatum. Mar. Chem.* 218:103735. doi: 10.1016/j.marchem.2019.103735

Lin, P., Xu, C., Zhang, S., Sun, L., Schwehr, K. A., Bretherton, L., et al. (2017). Importanceof coccolithophore-associated organic biopolymers for fractionating particle-reactive radionuclides (^{234}Th, ^{233}Pa, ^{210}Pb, ^{210}Po, and ^{7}Be) in the ocean. *J. Geophys. Res. Biogeosci.* 122, 2033–2045. doi: 10.1002/2017jg003779

Moran, S. B., Weinstein, S. E., Edmonds, H. N., Smith, J. N., Kelly, R. P., Pilson, M. E. Q., et al. (2003). Does ^{234}Th/^{238}U and disequilibrium provide an accurate record of the export flux of and particulate organic carbon from the upper ocean. *Limnol. Oceanogr.* 48, 1018–1029. doi: 10.4319/lo.2003.48.3.1018

Murray, J. W., Paul, B., Dunne, J. P., and Chapin, T. (2005). ^{234}Th, ^{210}Pb, ^{210}Po and stable Pb in the central equatorial Pacific: tracers for particle cycling. *Deep Sea Res. I Oceanogr. Res. Papers* 52, 2109–2139. doi: 10.1016/j.dsr.2005.06.016

Nelson, D. M., Treguer, P., Brzezinski, M. A., Leynaert, A., and Queguiner, B. (1995). Production and dissolution of biogenic silica in the ocean-revised global estimates, comparison with regional data and relationship to biogenic sedimentation. *Glob. Biogeochem. Cycles* 9, 359–372. doi: 10.1029/95gb01070

Quigg, A., Passow, U., Chin, W.-C., Bretherton, L., Kamalanathan, M., Xu, C., et al. (2016). The role of microbial exopolymers in determining the fate of oil and chemical dispersants in the ocean. *Limnol. Oceanogr. Lett.* 1, 3–26. doi: 10.1002/lol2.10030

Quigley, M. S., Santschi, P. H., Hung, C.-C., Guo, L., and Honeyman, B. D. (2002). Importance of acid polysaccharides for ^{234}Th complexation to marine organic matter. *Limnol. Oceanogr.* 47, 367–377. doi: 10.4319/lo.2002.47.2.0367

Roberts, K. A., Xu, C., Hung, C.-C., Conte, M. H., and Santschi, P. H. (2009). Scavenging and fractionation of thorium vs. protactinium in the ocean, as determined from particle-water partitioning experiments with sediment trap material from the Gulf of Mexico and Sargasso Sea. *Earth Planet. Sci. Lett.* 286, 131–138. doi: 10.1016/j.epsl.2009.06.029

Roy-Barman, M., Lemaître, C., Ayrault, S., Jeandel, C., Souhaut, M., and Miquel, J.-C. (2009). The influence of particle composition on Thorium scavenging in the Mediterranean Sea. *Earth Planet. Sci. Lett.* 286, 526–534. doi: 10.1016/j.epsl.2009.07.018

Santschi, P. H., Adler, D., Amdurer, V. M., Li, Y.-H., and Bell, J. J. (1980). Thorium isotopes as analogs for particle-reactive pollutants in coastal marine environments. *Earth Planet. Sci. Lett.* 47, 327–335. doi: 10.1016/0012-821x(80)90019-9

Santschi, P. H., Balnois, E., Wilkinson, K. J., Zhang, J., and Buffle, J. (1998). Fibrillar polysaccharides in marine macromolecular organic matter as imaged by atomic force microscopy and transmission electron microscopy. *Limnol. Oceanogr.* 43, 896–908. doi: 10.4319/lo.1998.43.5.0896

Santschi, P. H., Xu, C., Schwehr, K. A., Lin, P., Sun, L., Chin, W.-C., et al. (2020). Can the protein/carbohydrate (P/C) ratio of exopolymeric substances (EPS) be used as a proxy for their 'stickiness' and aggregation propensity? *Mar. Chem.* 218:103734. doi: 10.1016/j.marchem.2019.103734

Shimmield, G. M., Ritchie, G. D., and Fileman, T. W. (1995). The impact of marginal ice zone processes on the distribution of 210Pb, 210Po and 234Th and implications for new production in the Bellingshausen Sea, Antarctica. *Deep Sea Res. II* 42, 1313–1335. doi: 10.1016/0967-0645(95)00071-w

Stewart, G. M., Cochran, J. K., Miquel, J. C., Masque, P., Szlosek, J., Rodriguez y Baena, A. M., et al. (2007a). Comparing POC export from ^{234}Th/^{238}U and ^{210}Po/^{210}Pb disequilibria with estimates from sediment traps in the northwest Mediterranean. *Deep-Sea Res. I* 54, 1549–1570. doi: 10.1016/j.dsr.2007.06.005

Stewart, G. M., Cochran, J. K., Xue, J., Lee, C., Wakeham, S. G., Armstrong, R. A., et al. (2007b). Exploring the connection between ^{210}Po and organic matter in the northwestern Mediterranean. *Deep Sea Res. I Oceangr. Res. Papers* 54, 415–427. doi: 10.1016/j.dsr.2006.12.006

Stewart, G. M., Fowler, S. W., Teyssle, J. L., Cotret, O., Cochran, J. K., and Fisher, N. S. (2005). Contrasting transfer of polonium-210 and lead-210 across three trophic levels in marine plankton. *Mar. Ecol. Prog. Series* 290, 27–33. doi: 10.3354/meps290027

Stewart, G. M., Moran, S. B., and Lomas, M. W. (2010). Seasonal POC fluxes at BATS estimated from ^{210}Po deficits. *Deep Sea Res. I* 57, 113–124. doi: 10.1016/j.dsr.2009.09.007

Stewart, G. M., Moran, S. B., Lomas, M. W., and Kelly, R. P. (2011). Direct comparison of ^{210}Po, ^{234}Th and POC particle-size distributions and export fluxes at the Bermuda Atlantic Time-series Study (BATS) site. *J. Environ. Radioact.* 102, 479–489. doi: 10.1016/j.jenvrad.2010.09.011

Stubbins, A., Spencer, R. G. M., Chen, H., Hatcher, P. G., Mopper, K., Hernes, P. J., et al. (2010). Illuminated darkness: molecular signatures of Congo River dissolved organic matter and its photochemical alteration as revealed by ultrahigh precision mass spectrometry. *Limnol. Oceanogr.* 55, 1467–1477. doi: 10.4319/lo.2010.55.4.1467

Verdeny, E., Masque, P., Garcia-Orellana, J., Hanfland, C., Cochran, J. K., and Stewart, G. M. (2009). POC export from ocean surface waters by means of ^{234}Th/^{238}U and ^{210}Po/^{210}Pb disequilibria: a review of the use of two radiotracer pairs. *Deep Sea Res. II Top. Stud. Oceangr.* 56, 1502–1518. doi: 10.1016/j.dsr2.2008.12.018

Wei, C.-L., Lin, S.-Y., Sheu, D. D.-D., Chou, W.-C., Yi, M.-C., Santschi, P. H., et al. (2011). Particle-reactive radionuclides (^{234}Th, ^{210}Pb, ^{210}Po) as tracers for the estimation of export production in the South China Sea. *Biogeosciences* 8, 3793–3808. doi: 10.5194/bg-8-3793-2011

Xu, C., Lin, P., Sun, L., Chen, H., Hatcher, P. G., Conte, M. H., et al. (2020). Molecular nature of marine particulate organic iron-carrying moieties revealed by Fourier-Transform Ion Cyclotron Resonance Mass Spectrometry (ESI-FTICRMS). *Front. Earth Sci.* 8:266. doi: 10.3389/feart.2020.00266

Xu, C., Santschi, P. H., Hung, C.-C., Zhang, S., Schwehr, K. A., Roberts, K. A., et al. (2011a). Controls of ^{234}Th removal from the oligotrophic ocean by polyuronic acids and modification by microbial activity. *Mar. Chem.* 123, 111–126. doi: 10.1016/j.marchem.2010.10.005

Xu, C., Zhang, S., Chuang, C.-Y., Miller, E. J., Schwehr, K. A., and Santschi, P. H. (2011b). Chemical composition and relative hydrophobicity of microbial exopolymeric substances (EPS) isolated by anion exchange chromatography and their actinide-binding affinities. *Mar. Chem.* 126, 27–36. doi: 10.1016/j.marchem.2011.03.004

Xu, C., Zhang, S. J., Kaplan, D. I., Ho, Y. F., Schwehr, K. A., Roberts, K. A., et al. (2015). Evidence for hydroxamate siderophores and other n-containing organic compounds controlling (Pu)-239,240 immobilization and remobilization in a wetland sediment. *Environ. Sci. Technol.* 49, 11458–11467. doi: 10.1021/acs.est.5b02310

Yang, W., Huang, Y., Chen, M., Qiu, Y., Li, H., and Zhang, L. (2011). Carbon and nitrogen cycling in the Zhubi coral reef lagoon of the South China Sea as revealed by ^{210}Po and^{210}Pb. *Mar. Pollut. Bull.* 62, 905–911. doi: 10.1016/j.marpolbul.2011.02.058